

ESTIMATION AND CORRELATION OF SURFACE WATER VAPOUR DENSITY IN BENIN, NIGERIA

ABSTRACT

The present study investigated the monthly average daily mean temperature, relative humidity, surface pressure, cloud cover, and sunshine hours associated with monthly variations in surface water vapour density (SWVD) for the period extending from 1979 to 2016) for Benin (Latitude 6.32⁰N, Longitude 5.10⁰E). The daily variation of SWVD for the dry season (November to March) and rainy season (April to October) for the year 2014 was examined. Statistical indices of coefficient of determination (R^2), mean bias error (MBE), root mean square error (RMSE), mean percentage error (MPE), Nash-Sutcliffe equation (NSE), and index of agreement (IA) were used to compare and evaluate the generated two variable SWVD-based models. The findings revealed that the level of SWVD varied throughout the investigation period on each day of the month. The SWVD is higher during the wet season than it is during the dry season, based to the monthly average daily values. The average SWVD was found to be at its highest point in the month of August during the rainy season and its lowest point in the month of December during the dry season (21.1448 gm⁻³). The greatest amount of SWVD was observed on 23rd May, 2014 with 27.57313 gm⁻³ and the lowest on 26th December, 2014 with 9.656676 gm⁻³. Pressure and precipitable water vapour are related to each other using a multivariate correlation regression model that was constructed with $R^2 = 100\%$, MBE = -0.0204 gm⁻³, RMSE = 0.0206 gm⁻³, MPE = 0.1105 %, NSE = 99.9897% and IA = 99.9974% was better appropriate for SWVD estimation with the best fitting and therefore can be used for estimating SWVD in Benin.

Keywords: Correlation models, dry Season, ECMWF, rainy season, SWVD

1. INTRODUCTION

Water vapour plays a very important function in studies on hydrological processes, climate change, weather systems and Earth's energy balance [1 – 4]. "The most common greenhouse gas in the atmosphere is the water vapour which accounts for approximately 60 % of the phenomenon of natural greenhouse effect" [1, 5]. At the surface, the water vapour which is also known as humidity is a key meteorological and climatological parameter that affects the comfort of human [6], also surface evaporation and plants' transpiration. The surface specific (q) and relative humidity (RH) are customarily measured using wet and dry bulb thermometers or RH sensors exposed in thermometer screens at meteorological or weather stations [7].

"Water has been seen as the fundamental of hydrological cycle, which is inter or intra/ within or outside movement of water in the atmosphere, oceans, rivers, and seas, as well as on land. Transfer of heat and energy between the earth's surface and the atmosphere and within the planet is possible due to hydrological cycle". [41] "Water vapour is the most effective and primary greenhouse gas in the atmosphere, as it absorbs long wave radiation

32 and radiates it back to the surface, which contributes to warming" [2, 8 – 11, 40]. "As the
 33 temperature of the Earth's surface and atmosphere increases, the atmosphere tends to hold
 34 more water vapour" [2]. "In the troposphere, water vapour molecules absorbed heat energy
 35 radiated from the Earth's surface" [12].

36 "The atmosphere tends to store more water vapour as the Earth's surface temperature rises.
 37 As a result of this atmospheric water vapor's role as a greenhouse gas, it absorbs energy
 38 that would otherwise reduce the amount of electromagnetic radiation that travels through the
 39 atmosphere, which could result in localised or global warming. Water vapour content in the
 40 air at ground level varies from less than 0.001% in the arctic to more than 6% in the tropics
 41 on average" [13 – 14]. "This amount decreases rapidly with height" [13].

42 "One of the most complex and difficult scientific issues facing the climate science community
 43 today is understanding the mechanisms that control the natural stability and changes in the
 44 climate system. Because of this, human actions that cause external forcing, such as the
 45 emission of greenhouse gases and changes in land use, are only partially predicted" [15 -
 46 16]. This is so because scientists lack the ability to actually do so since they cannot foretell
 47 population change, economic change, technological development and other relevant
 48 characteristic of future human activities [16].

49 The present study investigates the SWVD variation on a daily and monthly scale, as well as
 50 an analysis of the monthly variation using meteorological indicators for Benin, an area in
 51 South Western Nigeria. Two variable correlation models for estimating SWVD for the site
 52 were also constructed as part of the study.

53 2. METHODOLOGY

54

55 The European Centre for Medium-Range Weather Forecasts (ECMWF) at 2 m height
 56 provided the daily and monthly meteorological data for Benin, Nigeria, which are the average
 57 minimum temperature, maximum temperature, relative humidity, surface pressure, cloud
 58 cover, and sunshine hours that were used in this study. The study period is for 38 years
 59 extending from 1979 to 2016.

60 The following expression relates the surface water vapour density (SWVD), vapour pressure
 61 (e), and mean temperature (T) [1, 14, 16] as:

62

$$63 \quad SWVD = 216.7 \left(\frac{e}{T} \right) \quad (1)$$

64 They also obtained vapour pressure (e) using the expression as

$$65 \quad e = RH \left(\frac{e_s}{100} \right) \quad (2)$$

66 where RH and e_s stand for saturated vapour pressure and relative humidity, respectively.
 67 The Clausius Clapeyron equation was used to calculate the saturation vapour pressure [1,
 68 14, 16] defined as:

$$69 \quad \log_{10} e_s = 9.4051 - \left(\frac{2353}{T} \right) \quad (3)$$

70 The mean temperature T , was also obtained using [17]

$$71 \quad T = \frac{T_{max} + T_{min}}{2} \quad (4)$$

72 T_{max} and T_{min} are the maximum and minimum temperatures respectively. The SWVD is in
 73 gm^{-3} and e and e_s are in millibars (mb), T and RH are in Kelvin (K) in percentage (%)
 74 respectively.

75 The ambient Temperature T and Partial Pressure P_s are related by a correlation model as
 76 reported by [1] which is expressed by the semi empirical equation

$$77 \quad P_s = \exp \left(26.23 - \frac{5416}{T} \right) \quad (5)$$

78 The precipitable water in terms of relative humidity is presented with the following formula
 79 [18].

$$80 \quad W = \frac{(0.493 \phi_r P_s)}{T} \quad (6)$$

81 where φ_r is relative humidity in fractions of one, T and p_s are the ambient temperature and
 82 partial pressure of water vapour in saturated air respectively.

83 Then dew point temperature T_{dew} was estimated using [19]

$$84 \quad T_{dew} = T - \frac{100 - RH}{5} \quad (7)$$

85 where T and RH are the mean temperature (Kelvin) and relative humidity (%).

86 The virtual temperature ($T_{virtual}$) was calculated using [20].

$$87 \quad T_{virtual} = \frac{T}{1 - \frac{e}{p}(1 - \epsilon)} \quad (8)$$

88 where e is the vapour pressure and ϵ is a constant given as 0.622

89 The potential temperature $T_{potential}$ was estimated using [20]

$$90 \quad T_{potential} = T_{mean} \left(\frac{p_0}{p} \right)^{\frac{R}{c_p}} \quad (9)$$

91 The expression (equation 9) is known as the Poisson's equation where p_0 is the standard
 92 pressure usually taken as 1000hPa and $\frac{R}{c_p} = 0.286$

93 **2.1 The Developed Two Variable Correlation Models**

94

95 The proposed two variable correlation models are of the form:

$$96 \quad SWVD = a + bP + cCC \quad (10)$$

$$97 \quad SWVD = a + bP + cSSH \quad (11)$$

$$98 \quad SWVD = a + bP + cPWV \quad (12)$$

99 where P, CC, SSH, and PWV stand for Surface Pressure, Cloud Cover, Sunshine Hours,
 100 and Precipitable Water Vapour, respectively, and a, b, and c are empirical constants.

101

102 **2.2 Validation of the Models**

103 The models are validated by testing statistically the Mean Bias Error (MBE), Root Mean
 104 Square Error (RMSE), Mean Percentage Error (MPE), Nash-Sutcliffe equation (NSE),
 105 Index of Agreement (IA) and coefficient of determination (R^2) for each of the models.
 106 According to [21 – 28], the expressions for the MBE, RMSE and MPE are given as follows.

$$107 \quad MBE = \frac{1}{n} \sum_{i=1}^n (SWVD_{i,cal} - SWVD_{i,mea}) \quad (13)$$

$$108 \quad RMSE = \left[\frac{1}{n} \sum_{i=1}^n (SWVD_{i,cal} - SWVD_{i,mea})^2 \right] \quad (14)$$

$$109 \quad MPE = \left(\frac{\frac{1}{n} \sum_{i=1}^n SWVD_{i,mea} - SWVD_{i,cal}}{SWVD_{i,mea}} \right) \cdot 100\% \quad (15)$$

$$110 \quad NSE = 1 - \frac{\sum_1^n (SWVD_{i,mea} - SWVD_{i,cal})^2}{\sum_1^n \left(SWVD_{i,mea} - \overline{SWVD_{i,meas}} \right)^2} \quad (16)$$

$$111 \quad IA = 1 - \frac{\sum_{i=1}^n (SWVD_{i,cal} - SWVD_{i,mea})^2}{\sum_{i=1}^n \left(|SWVD_{i,cal} - SWVD_{i,mea}| + \left| SWVD_{i,mea} - \overline{SWVD_{i,meas}} \right| \right)^2} \quad (17)$$

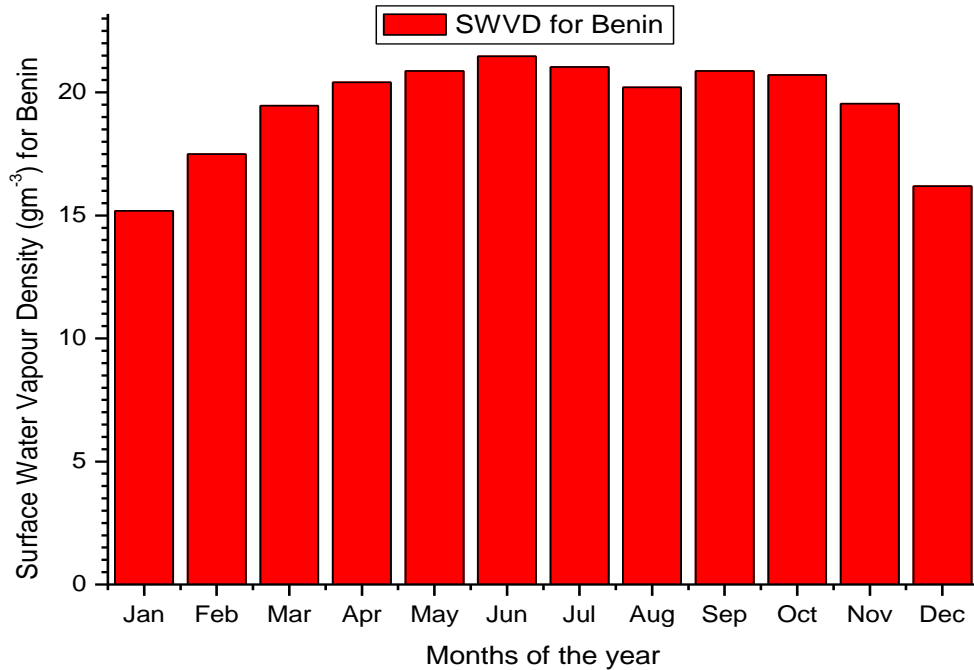
112 From equation (13) to (17) $SWVD_{i,cal}$, $SWVD_{i,mea}$ and n are the i^{th} calculated, i^{th} measured
 113 values of daily Surface Water Vapour Density and total number of observations respectively,
 114 also $\overline{SWVD_{i,meas}}$ is the mean Surface Water Vapour Density.

115 According to Chen et al. [29], an MBE value of zero is desirable. Furthermore, the
 116 performance of the model is improved by lower values for the MBE, RMSE, and MPE. MPE
 117 and MBE positive values denote overestimation, while MPE and MBE negative values
 118 denote underestimate. [30–35] The ideal percentage error range is between 10% and +10%.
 119 High R^2 , NSE, and IA values are preferred. While R^2 , MPE, NSE, and IA are expressed in
 120 percentage (%), the MBE and RMSE are expressed in gm^{-3} [36–39].

121 **3. RESULTS AND DISCUSSION**

122

123 **3.1 Surface Water Vapour Density and its Variation Meteorological Parameters for**
124 **Benin**



125

126

127

128

129

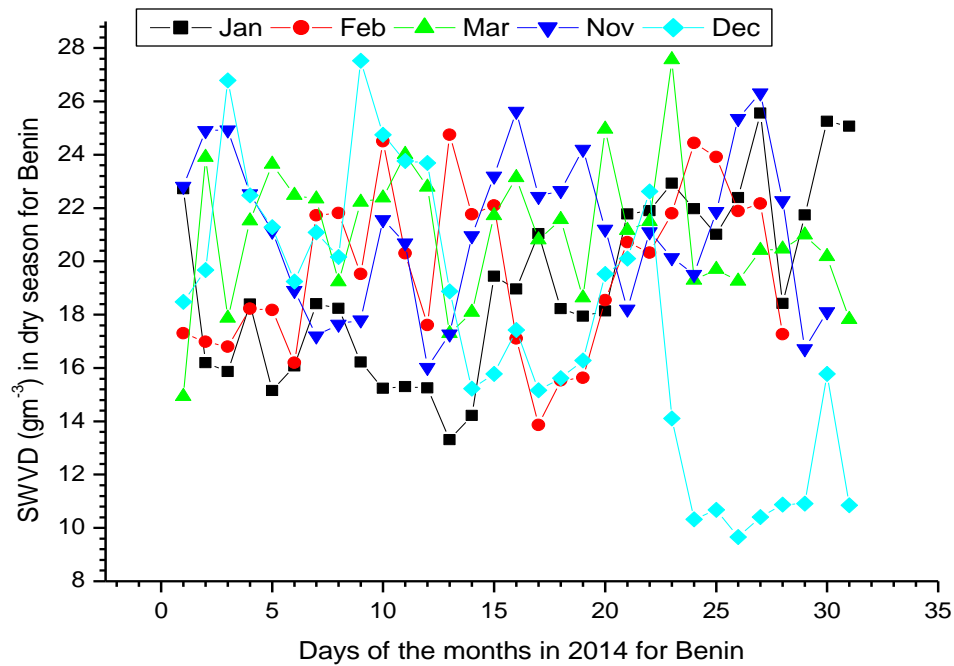
130

131

132

Fig. 1. Monthly variations of SWVD for Benin, Nigeria

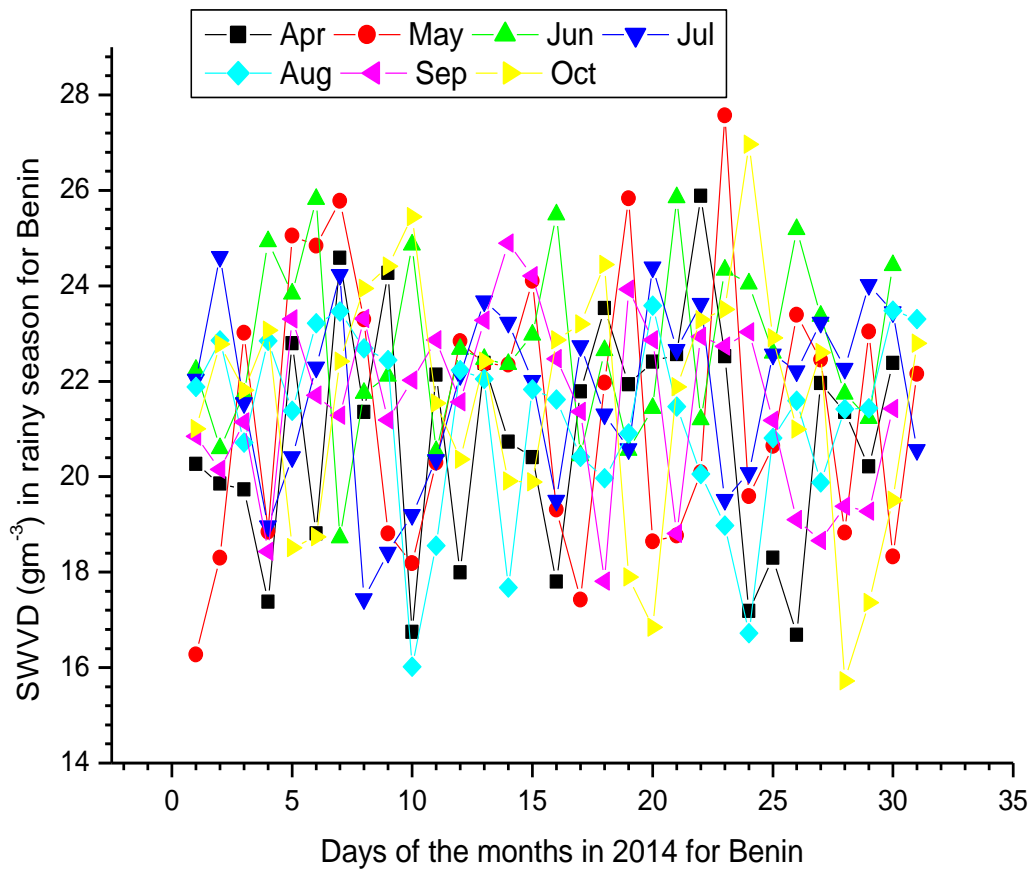
Fig. 1 shows the monthly variation of SWVD for Benin. The result indicated that the SWVD are higher in the rainy season is greater than in the dry season. It was observed that the maximum and minimum values of SWVD of 21.4753 gm⁻³ and 15.1798 gm⁻³ occurred in the months of June and January respectively. Furthermore, following its peak in June, SWVD drops in the months of July and August before increasing in the month of September. This discovery is consistent with the findings reported by Akpootu et al. [14] for Owerri, Nigeria.



133
134
135
136
137
138

Fig. 2. Diurnal variation of SWVD in the dry season for Benin Nigeria

Fig. 2 depicts the diurnal variation of SWVD specifically for the dry season in Benin. The outcome demonstrated variations in the SWVD quantity with the maximum and minimum values 27.5624 gm⁻³ and 9.6567 gm⁻³ on the 23rd March, 2014 and 26th December, 2014 respectively.

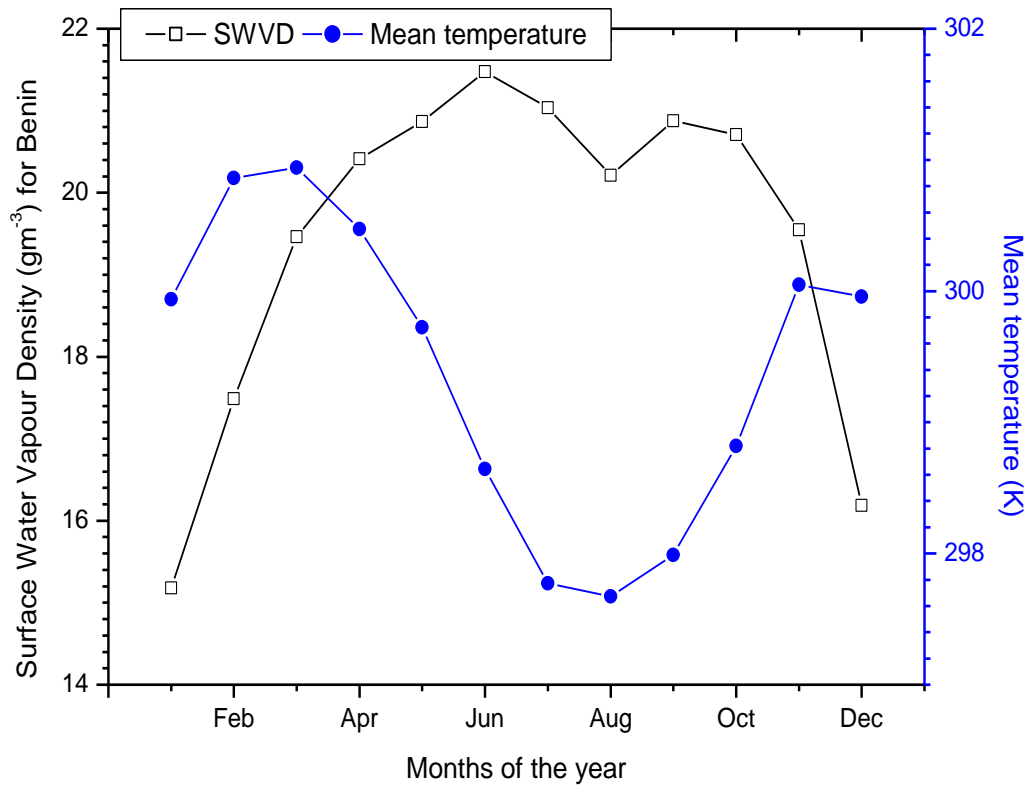


139
 140
 141
 142
 143
 144
 145
 146
 147
 148
 149

Fig. 3. Diurnal variation of SWVD in the rainy season for Benin Nigeria

Fig. 3 depicts the diurnal SWVD variation specifically for the rainy season in Benin. The result shows that the maximum the minimum values of SWVD occurred with 27.5731 gm⁻³ and 16.0151 gm⁻³ on the 23rd May, 2014 and 10th August, 2014 respectively.

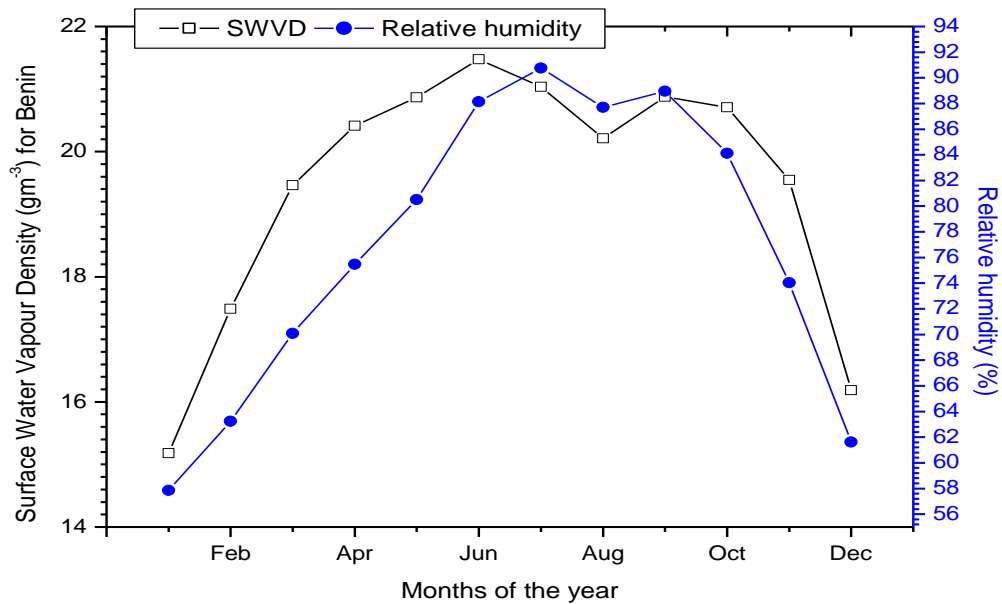
SWVD was determined to have an average value of 21.14479 gm⁻³. The SWVD's values fluctuate throughout the dry and wet seasons, according to the outcomes of its diurnal variations. Generally speaking, the 23rd of May 2014 marked the maximum value of surface water vapour density with 27.5731 gm⁻³ and the lowest on 26th December, 2014 with 9.6567 gm⁻³.



150
151
152
153
154
155
156
157
158
159
160
161

Fig. 4. Variation of SWVD with Mean Temperature for Benin

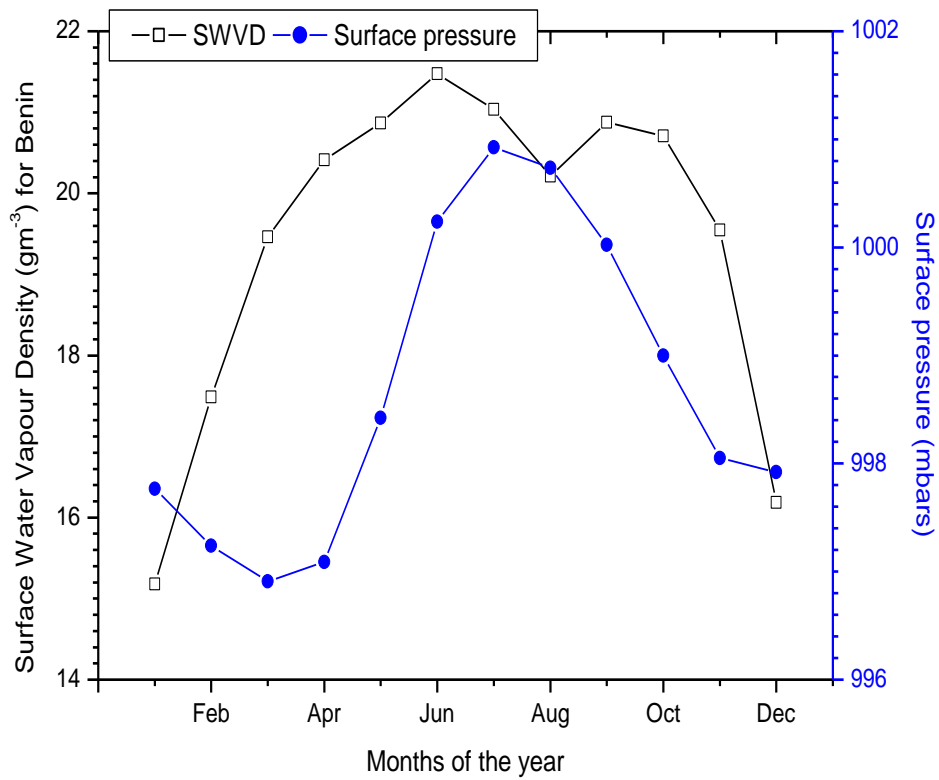
Benin's monthly seasonal variation in SWVD was shown in Fig. 4 together with the average temperature. The SWVD steadily grew from its lowest point of 15.1798 gm^{-3} in January to its highest point of 21.4753 gm^{-3} in June, then reduced in August with a dip downward that increased subsequently to September and finally dropped to December. The mean temperature rose along with the SWVD starting in January and peaked in March at 300.9395 K. It then fell until it reached its lowest point in August at 297.6724 K, before rising again to reach December. The short spell of dryness known as August Break, which coincided with the region's lowest temperature, may have contributed to the decline in SWVD that was reported in August. SWVD values were found to be high and low, respectively, during the dry and rainy seasons; while mean temperature indicated the opposite.



162
163
164
165
166
167
168

Fig. 5. Variation surface water vapour density with relative humidity for Benin

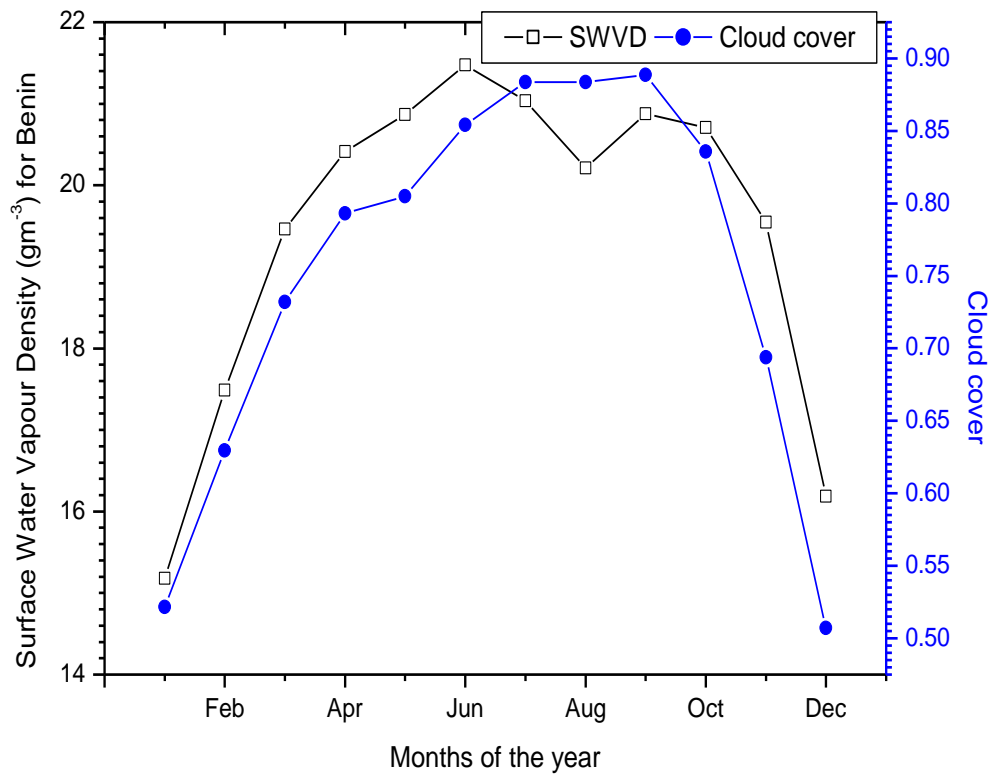
The monthly variation of SWVD with RH in Benin is depicted in Fig. 5. The outcome revealed that the relative humidity has increased by 57.8482% from its lowest point in January to its maximum value of 90.7671 % in July then drops down to August increases to September then dropped down to December with 61.6150 % the variation with SWVD is in phase therefore there was a close similarities between their characteristics.



169
 170
 171
 172
 173
 174

Fig. 6. Variation of SWVD with Surface Pressure for Benin

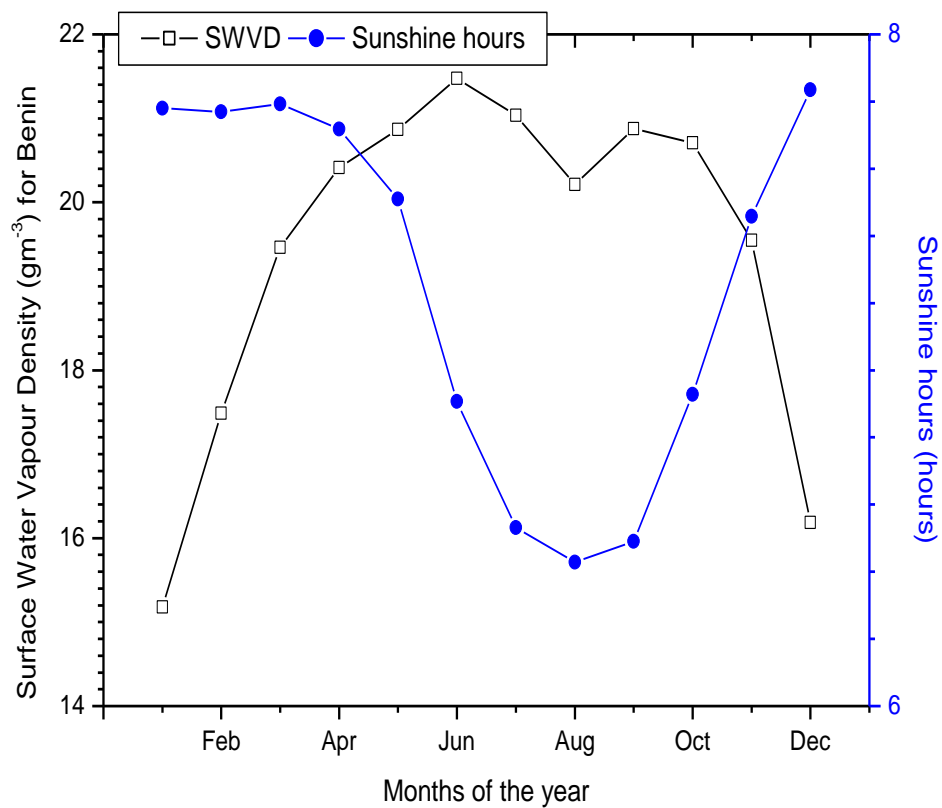
The fluctuation of SWVD with surface pressure is shown in Fig. 6; the result shows that the magnitude of surface pressure decreases from January to March then increases from April to March to its maximum value of 1000.9250 mbars in July then continue dropping to December. The minimum value of 996.9097 mbars was observed in March.



175
176
177
178
179
180
181

Fig. 7. Variation of SWVD with Cloud Cover for Benin

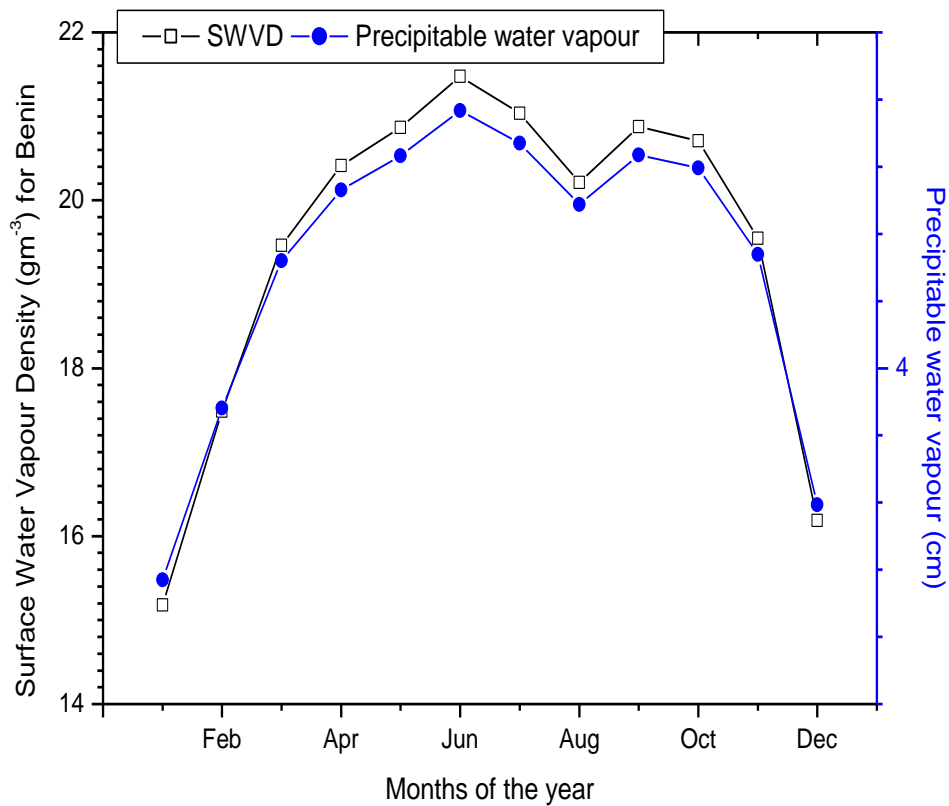
The seasonal variation of SWVD for Benin is depicted in Fig. 7 together with cloud cover. Both the cloud cover and SWVD increased from January to April with a little drop down in May then increase to July then continue, reaching to its highest level of 0.8886 in the month of September, and then decreased from October to its minimum value of 0.5070 in the month of December.



182
183
184
185
186
187
188
189

Fig. 8. Variation of SWVD with sunshine hours for Benin

The seasonal variation of SWVD for Benin is depicted in Fig. 8 together with sunshine hours. From January through May, the sunshine hours decline and increase at nearly equal intervals before decreasing to its minimum value in August (6.4278 hours), which coincided with the SWVD's August break. Sunshine hours rise from their lowest point in August to their highest point of 7.8356 hours in December. The outcome showed that, for SWVD, high and low values of sunshine hours were seen during the dry and wet seasons, respectively.

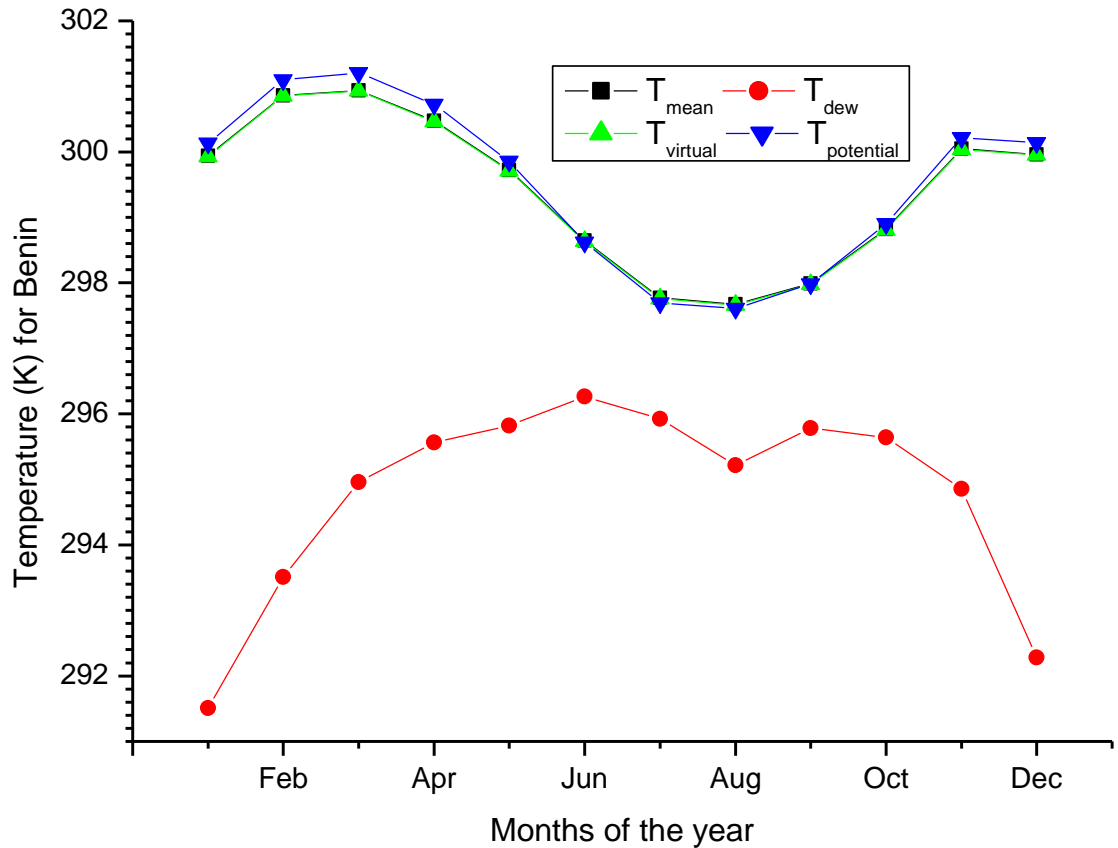


190
191
192
193
194
195
196
197
198
199

Fig. 9. Variation of SWVD with Precipitable Water Vapour for Benin

The seasonal variation of SWVD with Precipitable Water Vapour (PWV) is depicted in Figure 9. The result shows that the SWVD increase in the same pattern PWV they increase significantly from January until they reach their minimum value of 21.0359 gm⁻³ and 4.6697 cm in the month of July, the sudden drop in value of both the SWVD and the PWV in the month of August which is signified by the popular August break in the region.

3.2. Variation of Mean Temperature, Virtual Temperature, Potential Temperature and Dew Point Temperature for Benin



200
201
202
203
204
205
206
207
208
209
210
211
212
213
214
215
216
217
218
219
220
221

Fig. 10. Variation of SWVD with Temperature (T_m , T_p , T_v and T_d) for Benin

The seasonal change of the mean temperature, dew point temperature, virtual temperature, and potential temperature (T_d , T_v , T_p , and T_m) for Benin is depicted in Fig. 10. The result indicated that the mean temperature, the virtual temperature and potential temperature were almost the same and at the same rate of variation with SWVD, they all increase from January to their maximum values of 300.9395 K for mean temperature, 300.9292 K for virtual temperature and 301.2060 K for potential temperature. The temperatures continued to drop down from their maximum values to August where they also reached their minimum values of 297.6724 K for mean temperature, 297.6619 K for virtual temperature and 297.6096 for potential temperature. After the minimum level the temperatures rose to November then drop to December.

3.3. Two Variable Correlation Model for Benin

Based on equations 10 to 12, the two-variable correlation model generated for Benin is expressed as:

$$SWVD = 295 - 0.288P + 16.3CC \quad 18a$$

$$SWVD = 1053 - 1.00P - 4.80SSH \quad 18b$$

$$SWVD = 0.363 - 0.000364P + 4.51PWV \quad 18c$$

222 **Table 1a. Statistical validation tests for Benin**

Models	R ²	MBE	RMSE	MPE	NSE	IA
18a	92.5	0.1851	0.5714	-1.0531	96.5993	99.1695
18b	47.4	-0.0064	1.4271	-0.5888	78.7859	93.8017
18c	100	0.2882	0.2882	-1.4977	99.1346	99.7986

223

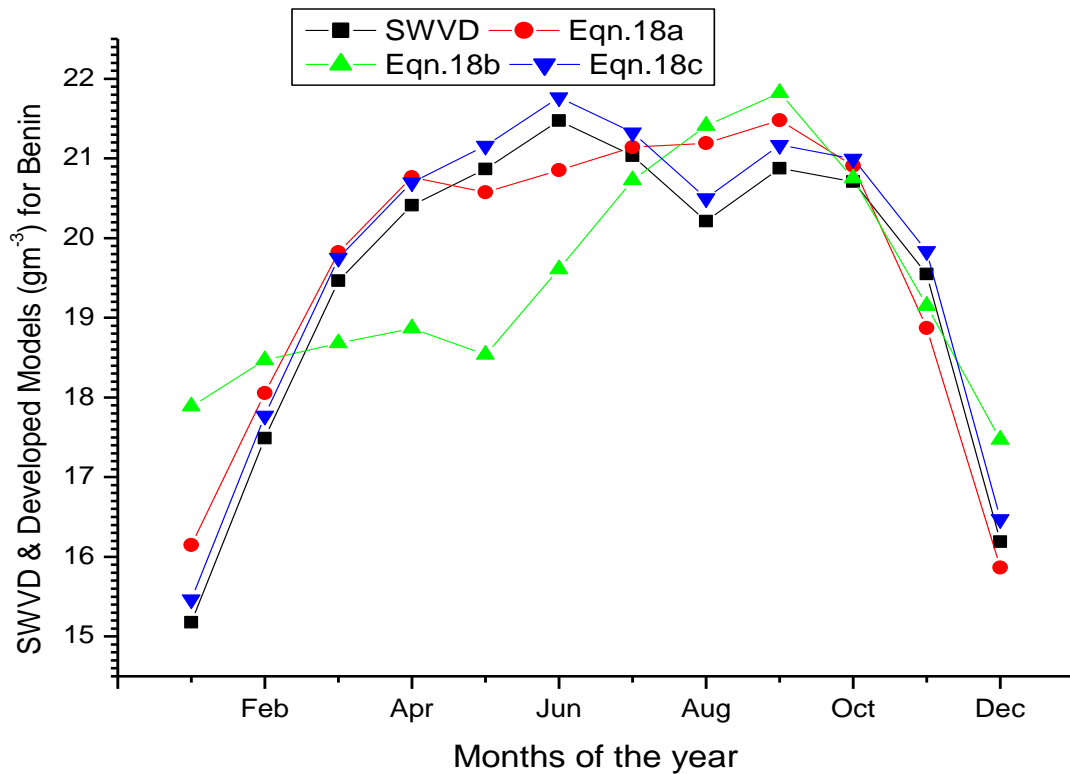
224 From table 1a above equation 18c has the highest R², NSE and IA it also has lowest RMSE
 225 which shows that it is the best equation for estimating SWVD in the location, but equation
 226 18b is the best in terms of MBE and MPE.

227 **Table 1b. ranking for the Models**

Models	R ²	MBE	RMSE	MPE	NSE	IA	Ranking
18a	2	2	2	2	2	2	12
18b	3	1	3	1	3	3	14
18c	1	3	1	3	1	1	10

228

229 The ranking from table 1b shows that both equation 18a and 18c are suitable for estimation
 230 of SWVD for Benin and stations with similar weather conditions, as they has equal and
 231 lowest ranking.



232

233

Fig. 11. Monthly variation of SWVD and developed models for Benin

234 Figure 11 shows the seasonal variation of SWVD with and the developed equations, the
235 result shows that equation 18b overestimates SWVD in January and February, then August
236 September and December. In addition, it undervalues it from March to July.

237 **4. CONCLUSION**

238

239 In the present study, data from the European Centre for Medium-Range Weather Forecasts
240 (ECMWF) for Benin, which is located in the Coastal region of Nigeria, were used to examine
241 the monthly SWVD and its change with other meteorological parameters throughout the
242 period spanning from 1979 to 2016. For the year 2014, the daily variance during the dry and
243 wet seasons was also examined. The R^2 , MBE, RMSE, MPE, NSE, and IA statistical indices
244 were used to assess three straightforward two-variable correlation models. It was found that
245 for the area, high SWVD values are recorded during the wet season and low SWVD values
246 during the dry season. Surface water vapour density peaked on May 23, 2014, with 27.5731
247 gm^{-3} , and it's lowest on December 26, 2014, with 9.6567 gm^{-3} . With the lowest RMSE and
248 maximum R^2 , NSE, and IA, the model that relates Pressure (P) with Precipitable Water
249 Vapour (PWV) was found to be the best for SWVD estimation in Benin.

250

251 **ACKNOWLEDGEMENTS**

252

253 The authors wish to thank the European Centre for Medium-Range Weather Forecasts
254 (ECMWF) for providing all the necessary meteorological data used in this study.

255

256

257 **COMPETING INTERESTS**

258

259 Authors have declared that no competing interests exist.

260

261 **AUTHORS' CONTRIBUTIONS**

262

263 This work was carried out in collaboration among all the authors. The data for the work was
264 sourced and analyzed by author DOA. Author MM and DOA supervised the work. The work
265 was drafted and edited by Author ZA. All the authors in this paper read and approved the
266 final manuscript.

267

268 **REFERENCES**

269

270 1. Akpootu DO, Iliyasu MI, Mustapha W, Salifu SI, Sulu HT, Arewa SP, Abubakar MB.
271 Models for Estimating Precipitable Water Vapour and Variation of Dew Point Temperature
272 with Other Parameters. Journal of Water Resources and Ocean Science. 2019a; 8(3), 28-36
273 doi: 10.11648/j.wros.20190803.11

274

275 2. Held IM, Soden BJ. Water vapour feedback and global warming, Annual Review of
276 Environment and Resources. 2000; vol. 25, pp. 441- 475.

277 3. Trenberth KE, Fasullo J, Smith L. Trends and variability in column-integrated atmospheric
278 water vapour. Climate Dynamics. 2005; vol. 24, no. 7-8, pp. 741-758.

279 4. Wang J, Carlson DJ, Parsons DB. Performance of operational radiosonde humidity
280 sensors in direct comparison with a chilled mirror dew-point hygrometer and its climate
281 implication. Geophysical Research Letters. 2003; vol. 30, no. 16.

282

283 5. Wagner T, Beirle S, Grzegorski M. Global trends (1996-2003) of total column precipitable
284 water observed by Global Ozone Monitoring Experiment (GOME) on ERS 2 and their

- 285 relation to near-surface temperature. *Journal of Geophysical Research: Atmospheres*. 2006;
286 vol. 111, no. 12, Article IDD12102.
287
- 288 6. Changnon DM, Sandstrom, C, Schaffer C, Relating changes in agricultural practices to
289 increasing dew points in extreme Chicago heat waves. *Climate Resources*. 2003; 24, 243–
290 254.
291
- 292 7. Dai A. Recent climatology, variability, and trends in global surface humidity. *Journal of*
293 *Climate Change*. 2006; vol. 19, no. 15: pp. 3589- 3606.
294
- 295 8. Zhao Y, Gong L, Zhou B, Huang Y, Liu C. Detecting tomatoes in greenhouse scenes by
296 combining AdaBoost classifier and colour analysis. *Biosyst. Eng*. 2016; 148, 127–137.
297
- 298 9. Dai A, Wang J, Thorne P. A new approach to homogenize daily radiosonde humidity data.
299 *Journal of Climate Change*. 2011; vol. 24, no. 4: pp. 965-991.
300
- 301 10. Khalameyda DD. Influence of fluctuations in the troposphere refractive index on the
302 interferometer measurement accuracy of radio wave angles of arrival. *Telecommun. Radio*
303 *Eng*. 70. 2011;
304
- 305 11. Khaniani AS, Nikraftar Z, Zakeri S. Evaluation of MODIS Near-IR water vapour product
306 over Iran using groundbased GPS measurements. *Atmospheric Resources*. 2020; 231,
307 104657.
308
- 309 12. Israel E, David AK, Samuel OO, Gabriel AA, Omolara EG. Global Distribution of Surface
310 Water Vapour Density Using in Situ and Reanalysis Data. *Journal of Water Resources and*
311 *Ocean Science*. 2020; 9(3), 64-70. doi: 10.11648/j.wros.20200903.12
312
- 313 13. Ajayi GO. Physics of the tropospheric radiopropagation. *Proceedings of the ICTP*
314 *College on Theoretical and Experimental Radio Propagation Physics*. 1989; 6–24, Trieste,
315 Italy.
316
- 317 14. Akpootu DO, Mustapha W, Rabiou AM, Iliyasu MI, Abubakar MB, Yusuf SO, Salifu SI.
318 Estimation of surface water Vapour Density and its Variation with other Meteorological
319 Parameters over Coastal region of Nigeria. *Hydrology*. 2019; 7(3), 46-55. DOI:
320 10.11648/j.hyd.20190703.12
321
- 322 15. IPCC. Intergovernmental Panel on Climate change. Third Assessment Report: Climate
323 change 2001. WG1: The scientific basis, summary for policymakers, Geneva, Switzerland.
324
- 325 16. Adeyemi B, Ogolo EO. Diurnal and Seasonal Variation of Surface Water Vapour Density
326 over some Meteorological Station in Nigeria. *Ife Journal of Science*. 2014; 16(2), 181-189.
327
- 328 17. Akpootu DO, Iliyasu MI, Nouhou I, Aina AO, Idris M, Mustapha W, Ohaji DE,
329 Muhammad AD. Estimation and Variation of Saturation Mixing Ratio and Mixing Ratio over
330 Potiskum, Nigeria. *Nigerian Journal of Basic and Applied Science*. 2022a; 30(1), 49-54. DOI:
331 <http://dx.doi.org/10.4314/njbas.v30i1.7>
332
- 332 18. Leckner B. The spectral distribution of solar radiation at the earth's surface—elements of
333 a model. *Sol Energy*. 1978; 20 (2), 143-150.
- 334 19. Lawrence MG. The relationship between relative humidity and the dewpoint temperature
335 in moist air: A simple conversion and applications. *Bull. Amer. Meteor. Soc.*, 2005; 86, 225-
336 233. doi: <http://dx.doi.org/10.1175/BAMS-86-2-225>.

- 337 20. Wallace JM, Hobbs PV. Atmospheric Science, An Introductory Survey, 2nd Edition,
338 Elsevier, 2006; pp 66-82.
- 339
340 21. El-Sebaili A, Trabea A. Estimation of Global Solar Radiation on Horizontal Surfaces over
341 Egypt, Egypt. J. Solids. 2005; 28(1): 163-175.
342
- 343 22. Gana NN, Akpootu DO. Angstrom Type Empirical Correlation for Estimating Global Solar
344 Radiation in North- Eastern Nigeria. The International Journal of Engineering And Science.
345 2013a; 2(11), 58-78. ISSN: 2319-1813
346
- 347 23. Gana NN, Akpootu DO. Estimation of global solar radiation using four sunshine based
348 models in Kebbi, North-Western, Nigeria. Pelagia Research Library. 2013b; 4(5), 409-421.
349 ISSN: 0976-8610.
350
- 351 24. Akpootu DO, Gana NN. Comparative Study of Global Solar Radiation between Nguru
352 and Abuja. A paper presented at the 24th Annual Congress and Colloquium of the Nigerian
353 Association of Mathematical Physics held at University of Benin, Benin City, Nigeria on the
354 25th-28th February, 2014. 2014;
355
- 356 25. Akpootu DO, Sanusi YA. A New Temperature-Based Model for Estimating Global Solar
357 Radiation in Port-Harcourt, South-South Nigeria. The International Journal of Engineering
358 And Science. 2015; 4(1), 63-73.
359
- 360 26. Olomiyesan BM, Akpootu DO, Oyedum DO, Olubusade JE, Adebunmi SO. Evaluation of
361 Global Solar Radiation Models Performance using Global Performance Indicator (GPI): A
362 Case Study of Ado Ekiti, South West, Nigeria. A paper presented at the 43rd Annual Nigerian
363 Institute of Physics, National Conference, held at the Nnamdi Azikiwe University, Awka,
364 Anambra State May 26-29, 2021. 2021;
- 365 27. Akpootu DO, Iliyasu MI. The Impact of some Meteorological Variables on the Estimation
366 of Global Solar Radiation in Kano, North Western, Nigeria. Journal of Natural Sciences
367 Research. 2015a; Vol.5, No.22, 1 – 13.
- 368 28. Akpootu DO, Iliyasu MI. A Comparative Study of some Meteorological Parameters for
369 Predicting Global Solar Radiation in Kano, Nigeria Based on Three Variable Correlations.
370 Advances in Physics Theories and Applications. 2015b; Vol.49, 1 – 9.
- 371
372 29. Chen R, Ersi K, Yang J. Validation of five global radiation Models with measured daily
373 data in China. Energy Conversion and Management. 2004; 45, 1759-1769.
374
- 375 30. Merges HO, Ertekin C, Sonmete MH. Evaluation of global solar radiation Models for
376 Konya, Turkey. Energy Conversion and Management. 2006; 47: 3149-3173.
- 377 31. Akpootu DO, Momoh M. Empirical Model for Estimating Global Solar Radiation in
378 Makurdi, Benue State, North Central Nigeria. A paper presented at the 36th Annual Nigerian
379 Institute of Physics, National Conference, held at the Department of Physics, University of
380 Uyo, Nigeria on May 26-29, 2014. 2014;
- 381 32. Akpootu DO, Sulu HT. A Comparative Study of Various Sunshine Based Models for
382 Estimating Global Solar Radiation in Zaria, North-Western, Nigeria. International Journal of
383 Technology Enhancements and Emerging Engineering Research. 2015; 3(12), 1 – 5.

- 384 33. Akpootu DO, Tijjani BI, Gana UM. Empirical models for predicting global solar radiation
385 using meteorological parameters for Sokoto, Nigeria. International Journal of Physical
386 Research. 2019c; 7(2): 48 – 60. DOI: 10.14419/ijpr.v7i2.29160
- 387 34. Akpootu DO, Tijjani BI, Gana UM. Sunshine and Temperature Dependent Models for
388 Estimating Global Solar Radiation Across the Guinea Savannah Climatic Zone of Nigeria.
389 American Journal of Physics and Applications. 2019d; 7(5): 125-135. doi:
390 10.11648/j.ajpa.20190705.15.
- 391 35. Akpootu DO, Tijjani BI, Gana UM. New temperature dependent models for estimating
392 global solar radiation across the midland climatic zone of Nigeria. International Journal of
393 Physical Research. 2019e; 7(2): 70 – 80. DOI: 10.14419/ijpr.v7i2.29214
- 394 36. Akpootu DO, Tijjani BI, Gana UM. New temperature dependent models for estimating
395 global solar radiation across the coastal climatic zone of Nigeria. International Journal of
396 Advances in Scientific Research and Engineering (ijasre). 2019f; 5(9): 126 – 141. DOI:
397 10.31695/IJASRE.2019.33523
- 398 37. Akpootu DO, Abdullahi Z. DEVELOPMENT OF SUNSHINE BASED MODELS FOR
399 ESTIMATING GLOBAL SOLAR RADIATION OVER KANO AND IKEJA, NIGERIA. FUDMA
400 Journal of Sciences (FJS). 2022; Vol. 6 No. 3, June, 2022, pp 290 – 300. DOI:
401 <https://doi.org/10.33003/fjs-2022-0603-1001>
- 402 38. Akpootu DO, Iliyasu MI, Olomiyesan BM, Fagbemi SA, Sharafa SB, Idris M, Abdullahi Z,
403 Meseke NO. MULTIVARIATE MODELS FOR ESTIMATING GLOBAL SOLAR RADIATION
404 IN JOS, NIGERIA. Matrix Science Mathematic (MSMK). 2022b; 6(1) 05-12. DOI:
405 <http://doi.org/10.26480/mkmk.01.2022.05.12>
- 406 39. Akpootu DO, Alaiyemola SR, Abdulsalam MK, Bello G, Umar M, Aruna S, Isah AK,
407 Aminu Z, Abdullahi Z, Badmus TO. Sunshine and Temperature Based Models for Estimating
408 Global Solar Radiation in Maiduguri, Nigeria. Saudi Journal of Engineering and Technology.
409 2023; 8(5): 82-90. DOI: 10.36348/sjet.2023.v08i05.001.
- 410 40. Solomon S, Rosenlof KH, Portmann RW, Daniel JS, Davis SM, Sanford TJ, Plattner GK.
411 Contributions of stratospheric water vapor to decadal changes in the rate of global warming.
412 Science. 2010 Mar 5;327(5970):1219-23.
- 413 41. Akpootu DO, Momoh M, Abdullahi Z, Umar M. Estimation of Surface Water Vapour
414 Density and its Variation with other Meteorological Parameters over Akure, Nigeria. Saudi J
415 Eng Technol. 2023;8(8):189-99.
- 416